

# DARK MATTER IN SUPERGRAVITY

R. Arnowitt, B. Dutta, and Y. Santoso

Department of Physics, Center for Theoretical Physics, Texas A&M University,  
College Station, TX 77843-4242, USA

**Abstract.** We consider neutralino-proton cross sections for halo dark matter neutralinos ( $\tilde{\chi}_1^0$ ) within the framework of supergravity models with R-parity invariance for models with universal soft breaking (mSUGRA) and models with nonuniversal soft breaking. The analysis includes the necessary corrections to treat the large  $\tan\beta$  region (i.e. L-R mixing in the squark and slepton mass matrices, loop corrections to the  $b$  and  $\tau$  masses, etc) and includes all coannihilation phenomena. For mSUGRA, dark matter detectors with current sensitivity are seen to be probing the region where  $\tan\beta \gtrsim 25$ ,  $\Omega_{\tilde{\chi}_1^0} h^2 < 0.1$ ,  $m_{\tilde{\chi}_1^0} \lesssim 90$  GeV, and for the light Higgs,  $m_h \lesssim 120$  GeV. Nonuniversal models can have a much larger cross section, and current detectors can probe part of the parameter space where  $\tan\beta \gtrsim 4$ . Minimum cross sections are generally greater than  $10^{-9}$  pb to  $10^{-10}$  pb for  $m_{1/2} < 600$  GeV (and hence accessible to planned future detectors), with the exception of a region when  $\mu < 0$  where for  $m_{1/2} \gtrsim 450$  GeV,  $4 \lesssim \tan\beta \lesssim 20$ , the cross section drops to a minimum of about  $1 \times 10^{-12}$  pb at  $m_{1/2} = 600$  GeV,  $\tan\beta \simeq 10$ . In this region, the gluino and squarks lie above 1 TeV, but should still be accessible to the LHC.

## 1 Introduction

If the dark matter that exists in the Milky Way is a supersymmetric weakly interacting particle (wimp), there are several ways in which it might be detected. Annihilation of two wimps in the halo might give rise to signals of gamma rays, anti-protons or positrons. Dark matter particles caught by the gravitational fields of the Sun or Earth would be expected to sink to the center, and there annihilate leading to neutrinos that might be detected on the surface of the earth. Finally direct detection of incident wimps from their scattering by nuclear targets on the Earth is possible. Of these, the last possibility appears most promising, and there are now a large number of detectors searching for supersymmetric wimps. We consider here what signals might be available within the framework of supergravity(SUGRA) models with grand unification of the gauge coupling constants at the GUT scale  $M_G \cong 2 \times 10^{16}$  GeV. There are three different types of SUGRA models currently being investigated, which differ by the mechanisms used to achieve supersymmetry(SUSY) breaking in the physical sector. These are gravity mediated SUGRA models, gauge mediated models, and anomaly mediated models. Of these, the gravity mediated models with R-parity invariance have the most robust candidate for particle dark matter, and we will restrict our discussion here to such models. In gravity mediated models, the dark matter particle is the lightest supersymmetric particle, the LSP, (absolutely stable

due to the R-parity invariance), and this is generally the lightest neutralino,  $\tilde{\chi}_1^0$ . The nucleus- $\tilde{\chi}_1^0$  scattering cross section contains a spin independent part and a spin dependent part. For heavy nuclear targets, the spin independent scattering dominates, and it is possible to extract from data the  $\tilde{\chi}_1^0$ -proton cross section,  $\sigma_{\tilde{\chi}_1^0-p}$ . There are a number of astronomical uncertainties, but making conventional assumptions, current detectors (DAMA, CDMS, UKCDM) are sensitive to halo  $\tilde{\chi}_1^0$  if

$$\sigma_{\tilde{\chi}_1^0-p} \gtrsim 1 \times 10^{-6} \text{pb} \quad (1)$$

and future detectors (GENIUS, Cryoarray) plan to achieve sensitivities of

$$\sigma_{\tilde{\chi}_1^0-p} \gtrsim (10^{-9} - 10^{-10}) \text{pb} \quad (2)$$

We discuss here how these sensitivities might relate to supergravity models. In particular, we consider the minimal supergravity GUT model (mSUGRA)[1] which has universal soft breaking masses at  $M_G$ , and nonuniversal soft breaking models[2] which allow nonuniversal Higgs masses and nonuniversal third generation squark and slepton masses at  $M_G$  (but keep the gaugino masses universal at  $M_G$ ). While the models are physically different, they lead to qualitatively similar results: Current detectors are sensitive to a significant part of the SUSY parameter space, and future detectors should be able to cover all of the parameter space, except for special regions where there is an accidental cancelation of terms making  $\sigma_{\tilde{\chi}_1^0-p}$  anomalously small. Each of the above models contains a number of arbitrary new parameters. In spite of this they can still make relevant predictions for two main reasons: (i) Using the renormalization group equations (RGE) starting from  $M_G$ , they allow for radiative breaking of  $SU(2) \times U(1)$  at the electroweak scale (and thus furnish a natural explanation for the Higgs mechanism); (ii) Along with being able to calculate  $\sigma_{\tilde{\chi}_1^0-p}$ , the models can also calculate the relic density of neutralinos, i.e.  $\Omega_{\tilde{\chi}_1^0} h^2$ , where  $\Omega_{\tilde{\chi}_1^0} = \rho_{\tilde{\chi}_1^0} / \rho_c$ ,  $\rho_{\tilde{\chi}_1^0}$  is the relic mass density of the  $\tilde{\chi}_1^0$ , and  $\rho_c = 3H_0/8\pi G_N$ . Here  $H_0 = h(100 \text{km/s Mpc})$  is the Hubble constant, and  $G_N$  is the Newton constant. Both of the above lead to important constraints on the SUSY parameter space. Thus one has that

$$\Omega_{\tilde{\chi}_1^0} h^2 \sim \left( \int_0^{x_f} dx \langle \sigma_{\text{ann}} v \rangle \right)^{-1} \quad (3)$$

where  $\sigma_{\text{ann}}$  is the annihilation cross section in the early universe,  $v$  is the relative neutralino velocity at annihilation, and  $\langle \dots \rangle$  means thermal average. The dominant Feynman diagrams for  $\sigma_{\text{ann}}$  and spin independent  $\sigma_{\tilde{\chi}_1^0-p}$  are shown in Fig.1, and roughly speaking  $\sigma_{\text{ann}}$  depends on the crossed diagrams relative to  $\sigma_{\tilde{\chi}_1^0-p}$ . Thus usually, then, when  $\sigma_{\tilde{\chi}_1^0-p}$  is large,  $\sigma_{\text{ann}}$  will also be large, and hence by Eq(3),  $\Omega_{\tilde{\chi}_1^0} h^2$  will be small. Thus lower bounds on  $\Omega_{\tilde{\chi}_1^0} h^2$  will produce upper bounds on  $\sigma_{\tilde{\chi}_1^0-p}$ . In the following, we will assume  $h = 0.70 \pm 0.07$  and for matter(m) and baryonic matter(b) the values  $\Omega_m = 0.3 \pm 0.1$ , and  $\Omega_b = 0.04$ . (This corresponds to a dark energy amount of  $\Omega_\Lambda \sim 0.65$ ). For the dark matter then one has  $\Omega_{\tilde{\chi}_1^0} = 0.26 \pm 0.10$ , and if one combines errors in quadrature,

one finds  $\Omega_{\tilde{\chi}_1^0} h^2 = 0.13 \pm 0.05$ . Since there is undoubtedly a large amount of systematic error in the above estimates, in the following we will assume the approximately  $2\sigma$  spread of

$$0.02 < \Omega_{\tilde{\chi}_1^0} h^2 < 0.25 \quad (4)$$

The lower bound of Eq.(4) lies somewhat below other estimates. However, it also allows for the possibility that not all the dark matter in the Galaxy are neutralinos (e.g. some may be machos). In addition to the above, there are accelerator bounds that constrain the SUSY parameter space. In the following we use the LEP bounds for the light Higgs ( $h$ ) of  $m_h > 104$  GeV for  $\tan\beta = 3$ ,  $m_h > 102$  GeV for  $\tan\beta = 5$  and for the light chargino  $m_{\tilde{\chi}_1^\pm} > 102$  GeV. (For  $\tan\beta > 5$ , the Higgs mass bounds do not restrict the parameter space significantly.) The Tevatron gives the gluino ( $\tilde{g}$ ) mass bound of  $m_{\tilde{g}} > 270$  GeV (for gluino and squarks nearly degenerate). In addition there is the CLEO measurement of the  $b \rightarrow s + \gamma$  decay. We take here a  $2\sigma$  range around the experimental central value of the  $b \rightarrow X_s + \gamma$  branching ratio[3]:

$$1.8 \times 10^{-4} < B(B \rightarrow X_s \gamma) < 4.5 \times 10^{-4} \quad (5)$$

Of the above, the most significant constraints come from the Higgs mass bounds and the  $b \rightarrow s\gamma$  branching ratio.

## 2 Theoretical Analysis

In order to get accurate results, it is necessary to include a number of corrections in the calculations. We list some of these here: (1) One needs to run the two loop gauge RGE and one loop Yukawa RGE from  $M_G = 2 \times 10^{16}$  GeV down to the electroweak scale, iterating to get a consistent SUSY mass spectrum. (2) Below the SUSY scale  $M_S$ , one runs the QCD RGE for contributions dominated by light quarks. (3) It turns out that results are somewhat sensitive to bounds on the Higgs mass  $m_h$ , and so one needs to use the one loop, two loop and pole mass corrections to accurately calculate the value of  $m_h$ . (4) L-R mixing in the sfermion mass matrices must be included. These are important for large  $\tan\beta$  and in the third generation. (5) One loop corrections to  $m_b$  and  $m_\tau$  are included. This is needed to get the correct value of the  $b$  and  $\tau$  Yukawa coupling constants, and again are important for large  $\tan\beta$ . (6) Leading order (LO)[4] and some next to leading order (NLO)[5] corrections to the  $b \rightarrow s\gamma$  decay are included. All of the above are under good theoretical control except perhaps for the  $b \rightarrow s\gamma$  constraint<sup>1</sup>. We note that we do not make any assumptions on

---

<sup>1</sup> Recent analyses[6] appear to have calculated the most important NLO corrections to the branching ratio for  $b \rightarrow s\gamma$  for large  $\tan\beta$ . These corrections have not been treated here, but will be included in [7] (where the bounds on  $m_h$  will also be updated). We do not believe this will effect the predictions of the maximum and minimum cross sections given below, but may modify which regions of parameter space get excluded.

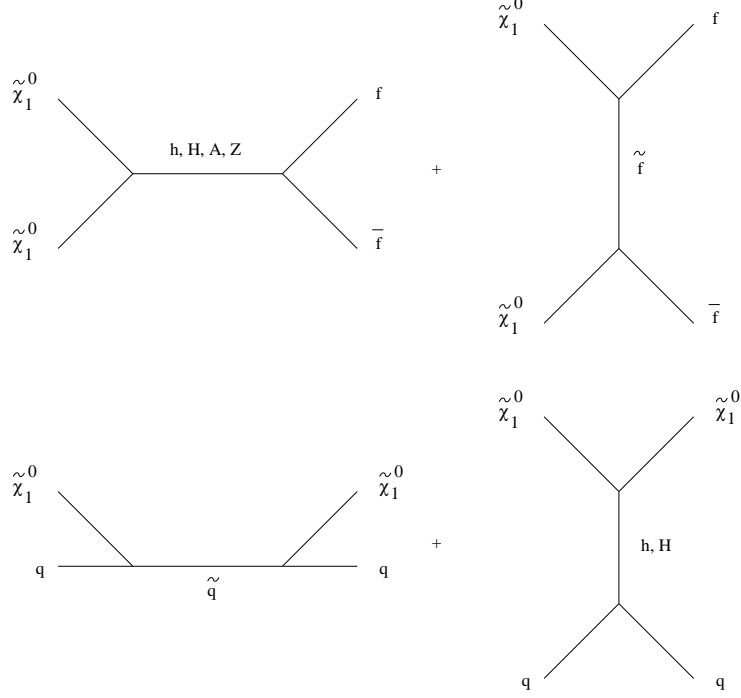


**Fig. 1.** Dominant diagrams for  $\sigma_{\text{ann}}$  (upper diagrams) and spin independent part of  $\sigma_{\tilde{\chi}_1^0-p}$  (lower diagrams).

the nature of the GUT group at grand unification. Hence we do not impose  $b - \tau$  (or  $b - \tau - t$ ) Yukawa unification at  $M_G$ , and do not impose proton decay constraints. Such phenomena depend sensitively on unknown post-GUT physics, and so the validity of these constraints are unclear. For example, string models in which there is Wilson line breaking of the GUT group to the Standard Model group at  $M_G$ , require gauge coupling constant unification but neither Yukawa unifications implied by the GUT group nor the SUGRA proton decay constraints need hold[8].

SUSY theory allows one to calculate neutralino-quark scattering (Fig.1), and one must convert this to neutralino-proton scattering to compare with experiment. To do this we follow the procedures of [9], which requires three parameters: (i) the pion-nucleon sigma term,  $\sigma_{\pi N} = 1/2(m_u + m_d) \langle p | u\bar{u} + d\bar{d} | p \rangle$ , (ii)  $\sigma_0 = \sigma_{\pi N} - (m_u + m_d) \langle p | s\bar{s} | p \rangle$ , and (iii) the quark mass ratio  $r = 2m_s/(m_u + m_d)$ . We use here the values  $\sigma_{\pi N} = 65$  MeV (based on analyses[10] making use of recent  $\pi - N$  scattering data),  $\sigma_0 = 30$  MeV [11], and  $r = 24.4 \pm 1.5$ [12]. If one were to use instead the value  $\sigma_{\pi N} = 45$  MeV (based on older  $\pi - N$  data) then the value of  $\sigma_{\tilde{\chi}_1^0-p}$  would be reduced by a factor of about 3.

### 3 mSUGRA Model

#### 3.1 Introduction

The mSUGRA model has universal soft breaking and so depends on a minimum number of new parameters i.e. four parameters and one sign. These are (1)  $m_0$ , the universal scalar particle mass at  $M_G$ . (2)  $m_{1/2}$ , the universal gaugino mass at  $M_G$ . (Alternately, one may use  $m_{\tilde{\chi}_1^0}$  or  $m_{\tilde{g}}$  since these scale approximately with  $m_{1/2}$ , i.e.  $m_{\tilde{\chi}_1^0} \simeq 0.4m_{1/2}$ , and  $m_{\tilde{g}} \simeq 2.8m_{1/2}$ ). (3)  $A_0$ , the universal cubic soft breaking mass at  $M_G$ . (4)  $\tan\beta = \langle H_2 \rangle / \langle H_1 \rangle$ , where  $\langle H_2 \rangle$  gives mass to the  $u$ -quarks and  $\langle H_1 \rangle$  gives mass to the  $d$ -quarks and charged leptons. In addition, the sign of the Higgs mixing parameter  $\mu$  is undetermined. ( $\mu$  appears in the superpotential  $W$  as  $\mu H_1 H_2$ .) We take for this parameter space the following ranges:

$$m_0 \leq 1 \text{ TeV} \quad (6)$$

$$m_{1/2} \leq 600 \text{ GeV (which corresponds to } m_{\tilde{g}} \leq 1.5 \text{ TeV, } m_{\tilde{\chi}_1^0} \leq 240 \text{ GeV)} \quad (7)$$

$$2 < \tan\beta < 50 \quad (8)$$

$$|A_0/m_0| \leq 5 \quad (9)$$

If one increases the  $m_{1/2}$  bound to  $m_{1/2} = 1 \text{ TeV}$  (corresponding to  $m_{\tilde{g}} = 2.5 \text{ TeV}$ , which is the upper detection limit for gluinos at the LHC), the neutralino-proton cross section will drop by a factor of about 2-3 at the high end of the parameter space.

#### 3.2 Maximum Cross Section

We examine first the maximum cross section the model can achieve.  $\sigma_{\tilde{\chi}_1^0-p}$  is an increasing function of  $\tan\beta$ , and a decreasing function of  $m_{1/2}$  and  $m_0$ . Thus the maximum  $\sigma_{\tilde{\chi}_1^0-p}$  should occur at large  $\tan\beta$  and small  $m_{\tilde{\chi}_1^0}$ . This is illustrated in Fig.2 where the maximum cross section is plotted as a function of  $m_{\tilde{\chi}_1^0}$  for  $\tan\beta = 20, 30, 40, 50$ , in the range of cross sections accessible to current detectors. One sees that current detectors with the sensitivity of Eq.(1), have begun to sample part of the parameter space for  $\tan\beta \gtrsim 25$ . Further, from the maximum  $\tan\beta = 50$  curve, one sees that only neutralinos with mass  $m_{\tilde{\chi}_1^0} \leq 90 \text{ GeV}$  are accessible to such detectors. Fig.3 shows  $\Omega_{\tilde{\chi}_1^0-p} h^2$  as a function of  $m_{\tilde{\chi}_1^0}$  for  $\tan\beta = 30$ , when  $\sigma_{\tilde{\chi}_1^0-p}$  takes on its maximum value of Fig.2. One sees that  $\Omega_{\tilde{\chi}_1^0} h^2$  is an increasing function of  $m_{\tilde{\chi}_1^0}$  as expected from the discussion in Sec.1, i.e. since  $\sigma_{\tilde{\chi}_1^0-p}$  decreases with  $m_{\tilde{\chi}_1^0}$ , one expects that the early universe annihilation cross will similarly decrease, and hence  $\Omega_{\tilde{\chi}_1^0} h^2$  will increase by Eq.(3). Since  $m_{\tilde{\chi}_1^0} \leq 90 \text{ GeV}$  for current detector sensitivities, we see that current detectors are accessing only the region where  $\Omega_{\tilde{\chi}_1^0} h^2 \leq 0.1$ . It is clear that the future very accurate determinations of  $\Omega_{\text{CDM}}$  by the MAP and Planck satellites will greatly sharpen the predictions of the SUGRA models. Fig.4 shows the light Higgs mass for  $\tan\beta = 30$  when  $\sigma_{\tilde{\chi}_1^0-p}$  takes on its maximum value. For  $m_{\tilde{\chi}_1^0} < 90 \text{ GeV}$  (the range

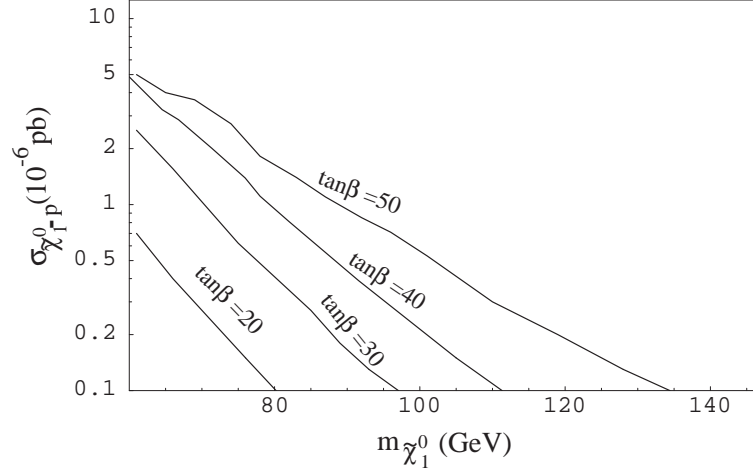


**Fig. 2.** Maximum  $\sigma_{\tilde{\chi}_1^0-p}$  as a function of  $m_{\tilde{\chi}_1^0}$  for  $\tan\beta = 20, 30, 40, 50$ , obtained by varying  $A_0$  and  $m_0$  over the parameter space[13]. The constraint on  $\Omega_{\tilde{\chi}_1^0} h^2$  of Eq.(4) has been imposed.

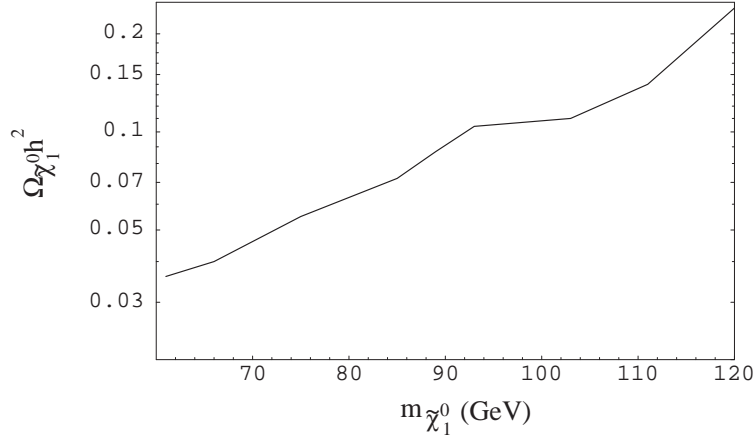


**Fig. 3.**  $\Omega_{\tilde{\chi}_1^0} h^2$  as a function of  $m_{\tilde{\chi}_1^0}$  for  $\tan\beta = 30$  when  $\sigma_{\tilde{\chi}_1^0-p}$  takes on its maximum value (as in Fig.2)[13].

accessible by current detectors) one has  $m_h \leq 120$  GeV. Such a range of Higgs mass would be accessible to RUN2 at the Tevatron, if the run achieves maximum luminosity.

### 3.3 Minimum Cross Sections

We turn next to consider how small the  $\sigma_{\tilde{\chi}_1^0-p}$  cross sections can get to see how sensitive future detectors must be to cover the full parameter space. It is

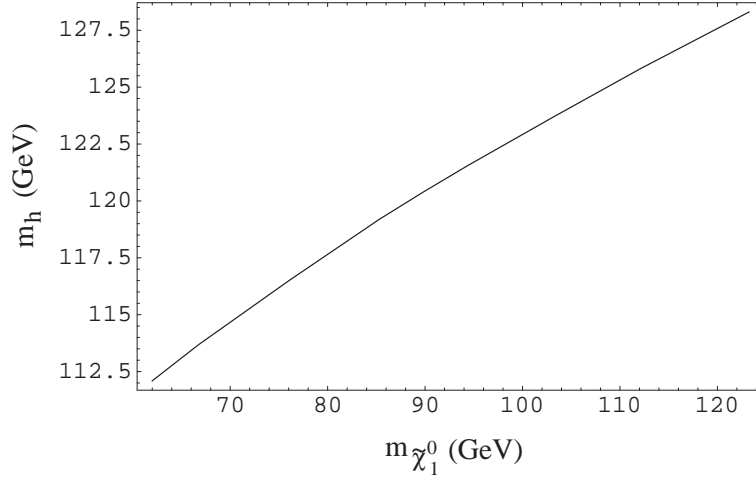


**Fig. 4.**  $m_h$  as a function of  $m_{\tilde{\chi}_1^0}$  for  $\tan\beta = 30$ , when  $\sigma_{\tilde{\chi}_1^0-p}$  takes on its maximum value[13].

convenient to divide the discussion into the region below coannihilation effects and the region where coannihilation can take place.

**Below coannihilation ( $m_{\tilde{\chi}_1^0} \leq 150$  GeV)** In this region there is no coannihilation, and the smallest cross sections occur at the smallest values of  $\tan\beta$ . Fig.5 shows the minimum value of the  $\sigma_{\tilde{\chi}_1^0-p}$  cross section as a function of  $m_{\tilde{\chi}_1^0}$  for  $\tan\beta=3$ . One sees that the cross section decreases with increasing  $m_{\tilde{\chi}_1^0}$  as

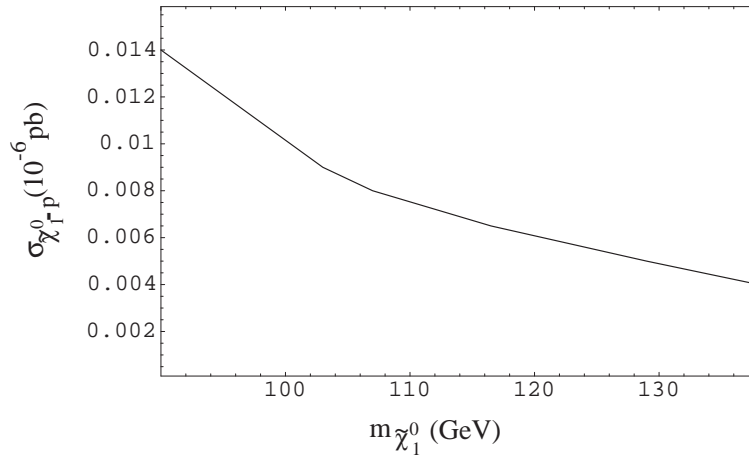


**Fig. 5.** Minimum  $\sigma_{\tilde{\chi}_1^0-p}$  for  $\tan\beta = 3$  for  $m_{1/2} < 345$  GeV[7].

expected, and in this domain we have

$$\sigma_{\tilde{\chi}_1^0 - p} \gtrsim 4 \times 10^{-9} \text{pb} \text{ for } m_{\tilde{\chi}_1^0} \leq 140 \text{ GeV}. \quad (10)$$

which would be accessible to planned future experiments (such as GENIUS).

**Coannihilation region ( $m_{\tilde{\chi}_1^0} \gtrsim 150 \text{ GeV}$ )** Coannihilation in the early universe occurs when a second SUSY particle becomes nearly degenerate with the neutralino LSP, and hence increase the annihilation cross section. This effect is significant in mSUGRA due to two “accidents”: (1) The  $\tilde{\chi}_1^0$  is a Majorana spinor and so its early universe annihilation cross section  $\sigma_{\tilde{\chi}_1^0 - \tilde{\chi}_1^0}$  is suppressed relative to e.g. R-slepton ( $\tilde{l}_R$ ) annihilations:

$$\sigma_{\tilde{\chi}_1^0 - \tilde{\chi}_1^0} \simeq (1/10)(\sigma_{\tilde{\chi}_1^0 - \tilde{l}_R}, \sigma_{\tilde{l}_R \tilde{l}_R}) \quad (11)$$

(2) There is an accidental near degeneracy between  $\tilde{l}_R$  and  $\tilde{\chi}_1^0$  in a small region of parameter space. To see this, one may look at low  $\tan\beta$ , where one has the analytic formulae for the selectron and neutralino masses of

$$m_{e_R}^2 = m_0^2 + (6/5)(\alpha_G/4\pi)f_1 m_{1/2}^2 - \sin^2 \theta_W M_W^2 \cos 2\beta \quad (12)$$

$$m_{\tilde{\chi}_1^0} \simeq (\alpha_1/\alpha_G)m_{1/2} \quad (13)$$

where  $f_1 = (1/\beta_1)[1 - (1/(1 + \beta_1 t))]$  and  $\beta_1$  is the  $U(1)$  beta function and  $t = 2\ln[M_G/M_Z]$ . Numerically, Eqs.(13) and (14) give

$$m_{e_R}^2 \simeq m_0^2 + 0.15m_{1/2}^2 + (40 \text{ GeV})^2 \quad (14)$$

$$m_{\tilde{\chi}_1^0}^2 \simeq 0.16m_{1/2}^2 \quad (15)$$

One sees that for small  $m_0$ , the  $\tilde{e}_R$  can become degenerate with the  $\tilde{\chi}_1^0$ , and as  $m_{1/2}$  increases,  $m_0$  correspondingly increases to maintain the region of near degeneracy. Thus one has a corridor in the  $m_0 - m_{1/2}$  plane of increasing  $m_0$  and  $m_{1/2}$  where coannihilation effects can occur, extending the region where Eq(4) can be satisfied. The importance of this effect has been stressed in [14], where the analysis has been carried out for low and intermediate  $\tan\beta$ , an example of which is shown in Fig.6. One sees that the coannihilation effect begins at  $m_{1/2} \gtrsim 400 \text{ GeV}$  (i.e.  $m_{\tilde{\chi}_1^0} \gtrsim 150 \text{ GeV}$ ). For large  $\tan\beta$ , the situation is more complicated as L-R mixing in the slepton mass matrices becomes important, particularly for the third generation, and generally the light  $\tilde{\tau}_1$  is the lightest slepton, considerably lighter than the other sleptons. We consider first the case where  $\mu > 0$ . (We use the Isajet sign convention for  $\mu$ ). Fig.7 shows the allowed region in the  $m_0 - m_{1/2}$  plane where Eq.(4) is satisfied for  $\tan\beta = 40$ . One sees that there is a significant  $A_0$  dependence, with larger  $A_0$  allowing for larger  $m_0$ . In general the thickness of the corridor is  $\delta m_0 \simeq 25 \text{ GeV}$ . There is no longer any non coannihilation region



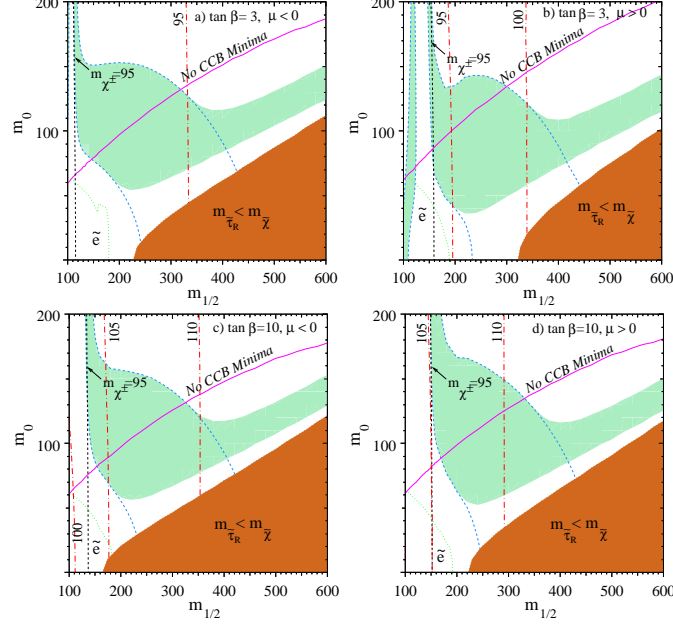
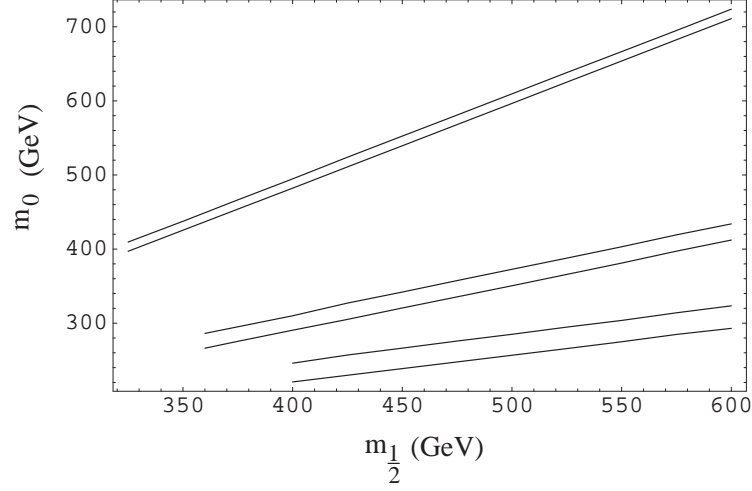


Figure 6: The light-shaded area is the cosmologically preferred region with  $0.1 \leq \Omega_\chi h^2 \leq 0.3$ . The light dashed lines show the location of the cosmologically preferred region if one ignores coannihilations with the light sleptons. In the dark shaded regions in the bottom right of each panel, the LSP is the  $\tilde{\tau}_R$ , leading to an unacceptable abundance of charged dark matter. Also shown are the isomass contours  $m_{\tilde{\chi}_\pm} = 95$  GeV and  $m_h = 95, 100, 105, 110$  GeV, as well as an indication of the slepton bound from LEP [31]. In the area below the solid contour, the scalar potential contains charge and/or colour breaking minima.

19

**Fig. 6.** Fig. 6 of Ellis et al[14]

left, as the corridors terminate at  $m_{1/2}$  above the non coannihilation domain (for large  $\tan \beta$ ). (The termination is due to the  $m_h$  and  $b \rightarrow s\gamma$  constraints.) The minimum value of  $m_{1/2}$  decreases with increasing  $A_0$ , as does the thickness of the allowed corridor. Thus for very large  $A_0$ , the existence of these corridors eventually becomes a fine tuning. Since larger values of  $A_0$  allow for larger values of  $m_0$ , one expects the  $\sigma_{\tilde{\chi}_1^0-p}$  cross section to decrease with  $A_0$ . This is illustrated in Fig.8 where  $\sigma_{\tilde{\chi}_1^0-p}$  is given as a function of  $m_{1/2}$  for  $\tan \beta = 40$  for two values of  $A_0$ . Thus one expects the minimum detection cross section to occur at largest  $A_0$  and smallest  $\tan \beta$ . This is illustrated in Fig.9. where the cross section is plotted for  $A_0 = 4m_{1/2}$ ,  $\mu > 0$ ,  $\tan \beta = 40$  and  $\tan \beta = 3$ . Because the higher  $\tan \beta$  allows  $m_0$  to become larger (compare with Fig.6) which also reduces the cross section, the  $\tan \beta$  dependence is mostly neutralized for large  $m_{1/2}$ . One has,



**Fig. 7.** Allowed corridors in  $m_0 - m_{1/2}$  plane satisfying the relic density constraint Eq(4) for  $\tan\beta=40$ ,  $\mu > 0$  and (from bottom to top)  $A_0 = m_{1/2}, 2m_{1/2}, 4m_{1/2}$  [7].

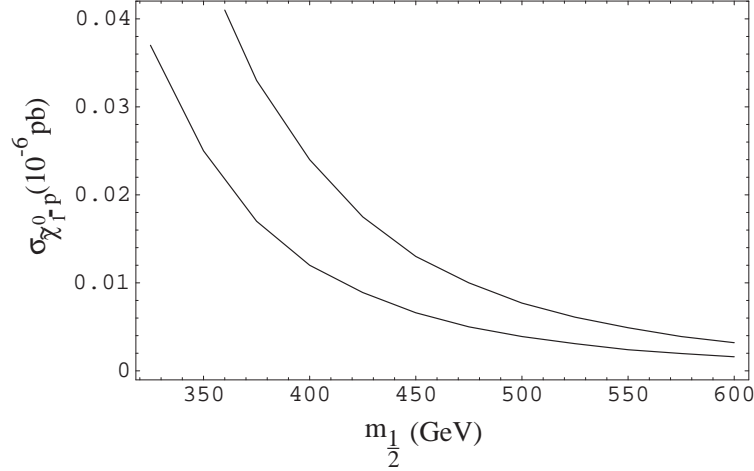


**Fig. 8.**  $\sigma_{\tilde{\chi}_1^0 - p}$  as a function of  $m_{1/2}$  for  $\tan\beta=40$ ,  $\mu > 0$ ,  $A_0 = 2m_{1/2}$  (upper curve) and  $A_0 = 4m_{1/2}$  (lower curve)[7].

however, the lower bound on the cross section of

$$\sigma_{\tilde{\chi}_1^0 - p} \gtrsim 1 \times 10^{-9} \text{ pb, for } m_{1/2} < 600 \text{ GeV } (m_{\tilde{\chi}_1^0} < 240 \text{ GeV}), \mu > 0 \quad (16)$$

which should still be accessible to the proposed future detectors.

We next turn to the case of  $\mu < 0$ . As pointed out in [15], at low and intermediate  $\tan\beta$ , an accidental cancellation can occur in part of the parameter space in the coannihilation region which can greatly reduce  $\sigma_{\tilde{\chi}_1^0 - p}$ . We investigate here whether this cancellation continues to occur in the high  $\tan\beta$  region.

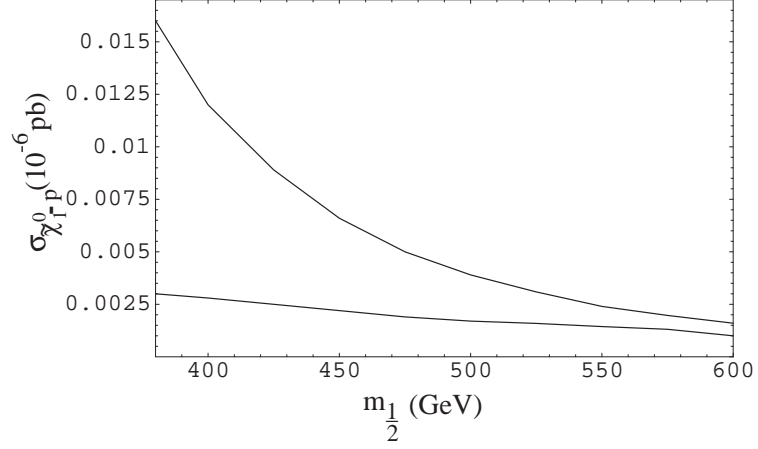


**Fig. 9.**  $\sigma_{\tilde{\chi}_1^0 p}$  as a function of  $m_{1/2}$  for  $A_0 = 4m_{1/2}$ ,  $\mu > 0$ ,  $\tan\beta = 40$  (upper curve),  $\tan\beta = 3$  (lower curve)[7].

What occurs is seen in Fig.10 where  $\sigma_{\tilde{\chi}_1^0 p}$  is shown for  $\tan\beta = 20, 5$  and  $10$  (in descending order). One sees that the cross section decreases between  $\tan\beta = 5$

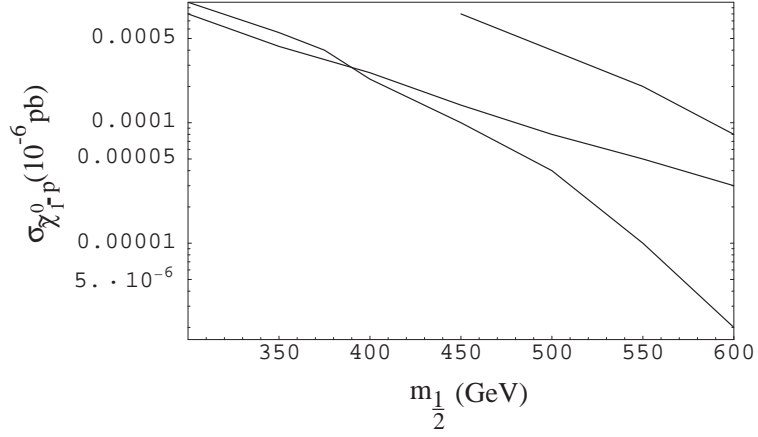


**Fig. 10.**  $\sigma_{\tilde{\chi}_1^0 p}$  for  $\mu < 0$ ,  $\tan\beta = 20, 5, 10$  (descending order on the right)[7].

and  $\tan\beta = 10$ , but then rises again at higher  $\tan\beta$ . Thus one has that

$$\sigma_{\tilde{\chi}_1^0 p} < 10^{-10} \text{ pb for } 4 \lesssim \tan\beta \lesssim 20; m_{1/2} > 450 \text{ GeV} (m_{\tilde{g}} \gtrsim 1.1 \text{ TeV}); \mu > 0 \quad (17)$$

and the minimum cross section occurs at  $\tan\beta \cong 10$ :

$$(\sigma_{\tilde{\chi}_1^0 p})_{\min} \simeq 1 \times 10^{-12} \text{ pb at } \tan\beta = 10, m_{1/2} \simeq 600 \text{ GeV} \quad (18)$$

Thus in this region of parameter space the proposed future detectors would not be able to detect mSUGRA  $\tilde{\chi}_1^0$  wimps. However, the absence of detection of halo wimps would then imply that squarks and gluinos should lie above 1 TeV, but at masses still accessible to the LHC. Also then, mSUGRA would require that  $\tan\beta$  would be in the restricted range given in Eq(18), and  $\mu$  be negative. This would allow a number of cross checks on the validity of the mSUGRA model.

## 4 Nonuniversal SUGRA Models

In most discussions of SUGRA models with nonuniversal soft breaking terms, the universality of the the soft breaking masses at  $M_G$  of the first two generations of squarks and sleptons is maintained to suppress flavor changing neutral currents. However, one may allow both the Higgs masses and the third generation squark and slepton masses to become nonuniversal at  $M_G$ . One can parameterize this situation at  $M_G$  as follows:

$$\begin{aligned} m_{H_1}^2 &= m_0^2(1 + \delta_1); & m_{H_2}^2 &= m_0^2(1 + \delta_2); \\ m_{q_L}^2 &= m_0^2(1 + \delta_3); & m_{t_R}^2 &= m_0^2(1 + \delta_4); & m_{\tau_R}^2 &= m_0^2(1 + \delta_5); \\ m_{b_R}^2 &= m_0^2(1 + \delta_6); & m_{l_L}^2 &= m_0^2(1 + \delta_7). \end{aligned} \quad (19)$$

where  $q_L \equiv (\tilde{t}_L, \tilde{b}_L)$  squarks,  $l_L \equiv (\tilde{\nu}_\tau, \tilde{\tau}_L)$  sleptons, etc. and  $m_0$  is the universal mass for the first two generations of squarks and sleptons. The  $\delta_i$  are the deviations from universality (and if one were to impose SU(5) or SO(10) symmetry one would have  $\delta_3=\delta_4=\delta_5$ , and  $\delta_6=\delta_7$ .) In the following we limit the  $\delta_i$  to obey:

$$-1 \leq \delta_i \leq +1 \quad (20)$$

and maintain gauge coupling constant unification and gaugino mass unification at  $M_G$ .

While there are a large numbers of new parameters, one can get an understanding of what effect they produce from the following. The neutralino  $\tilde{\chi}_1^0$  is a mixture of gaugino (mostly bino) and higgsino parts:

$$\tilde{\chi}_1^0 = \alpha \tilde{W}_3 + \beta \tilde{B} + \gamma \tilde{H}_1 + \delta \tilde{H}_2 \quad (21)$$

The dominant spin independent  $\sigma_{\tilde{\chi}_1^0-p}$  cross section is proportional to the interference between the gaugino and higgsino amplitudes, and this interference is largely governed by the size of  $\mu^2$ . As  $\mu^2$  decreases, the interference increases, and hence  $\sigma_{\tilde{\chi}_1^0-p}$  increases. Radiative breaking of  $SU(2) \times U(1)$  determines the value of  $\mu^2$  at the electroweak scale. To see the general nature of the effects of nonuniversality, we consider low and intermediate  $\tan\beta$  where an analytic form exists for  $\mu^2$  (see e.g. Arnowitt and Nath, Ref[2]):

$$\begin{aligned} \mu^2 &= \frac{t^2}{t^2 - 1} \left[ \left( \frac{1 - 3D_0}{2} - \frac{1}{t^2} \right) + \left( \frac{1 - D_0}{2} (\delta_3 + \delta_4) - \frac{1 + D_0}{2} \delta_2 + \frac{\delta_1}{t^2} \right) \right] m_0^2 \quad (22) \\ &+ \text{universal parts} + \text{loop corrections.} \end{aligned}$$

Here  $t = \tan\beta$  and  $D_0 \cong 1 - (m_t/200 \text{ GeV} \sin\beta)^2 \leq 0.2$  (Note that the Higgs and squark nonuniversality enter coherently, roughly in the combination  $\delta_3 + \delta_4 - \delta_2$ .) We see from Eq.(22) that  $\mu^2$  is reduced, and hence  $\sigma_{\tilde{\chi}_1^0-p}$  increased for  $\delta_3, \delta_4, \delta_1 < 0, \delta_2 > 0$ , and  $\mu^2$  is increased for  $\delta_3, \delta_4, \delta_1 > 0, \delta_2 < 0$ . Thus one can get significantly larger cross sections in the nonuniversal models with the first choice of signs for the  $\delta_i$ , and one can reduce the cross sections (though not by such a large amount) with the second choice. The above analytic results are illustrated in Fig.11, where the maximum  $\sigma_{\tilde{\chi}_1^0-p}$  for the universal and nonuniversal models are plotted for  $\tan\beta = 7$ . One sees that one can increase the cross section by a

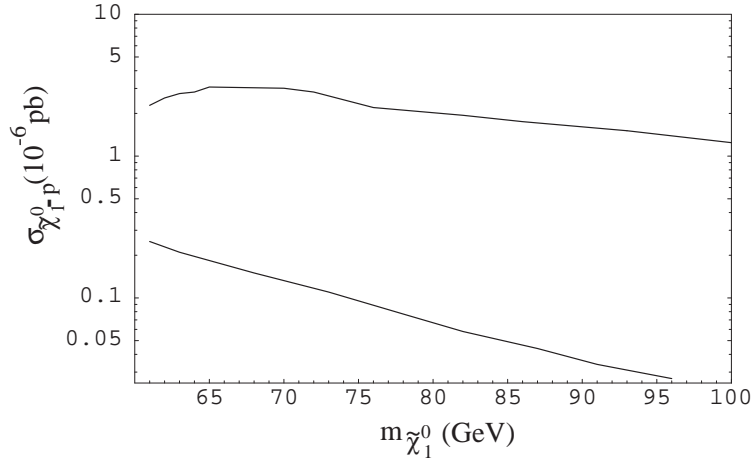


**Fig. 11.** Maximum  $\sigma_{\tilde{\chi}_1^0-p}$  for  $\tan\beta = 7, \mu > 0$  for nonuniversal model,  $\delta_3, \delta_4, \delta_1 < 0, \delta_2 > 0$  (upper curve), and universal model (lower curve)[13].

factor of 10 to 100 by an appropriate choice of signs. Thus current detectors can probe regions of lower  $\tan\beta$  for nonuniversal models than for the universal one. The allowed range can be seen from Fig.12, where the maximum cross sections are plotted for  $\tan\beta = 5, 7$ , and 15. Current detectors with sensitivity of Eq.(1) thus can probe parts of the parameter space with  $\tan\beta \gtrsim 4$ , and from the  $\tan\beta = 15$  curve, we see that parts of the high  $\tan\beta$  part of the parameter space has already been eliminated. However, the very low  $\tan\beta$  values are on the edge of being eliminated by the LEP constraint on the light Higgs mass. Thus Fig.13 shows that  $m_h$  is quite small if  $m_{\tilde{\chi}_1^0}$  is light, and one would have to raise the lower bound on  $\tan\beta$  as LEP raises the lower bound on  $m_h$ .

As in mSUGRA, the minimum cross sections occur for the largest  $m_{1/2}$  and smallest  $\tan\beta$ , and so they occur in the coannihilation region. We consider here only the case where the Higgs masses are nonuniversal i.e.  $\delta_{1,2} \neq 0$  (the other  $\delta_i$  set to zero). Results then are similar to the mSUGRA case. For  $\mu > 0$  we find

$$\sigma_{\tilde{\chi}_1^0-p} \gtrsim 1 \times 10^{-9} \text{ pb}; \text{ for } m_{1/2} \leq 600 \text{ GeV}, \mu > 0 \quad (23)$$

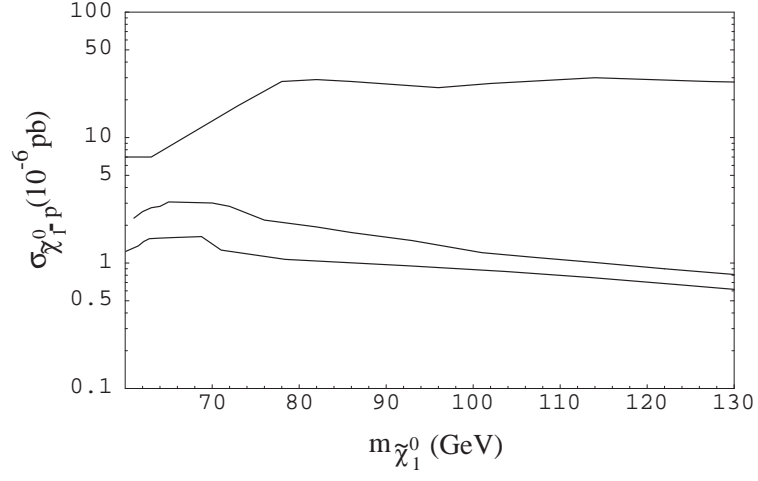


**Fig. 12.** Maximum  $\sigma_{\tilde{\chi}_1^0-p}$  for nonuniversal SUGRA models for  $\tan\beta=5,7$  and 15 (in ascending order)[13].

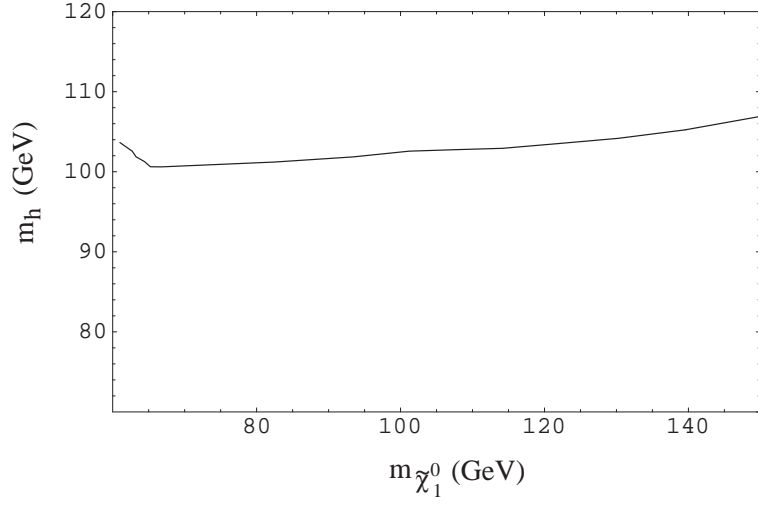


**Fig. 13.**  $m_h$  as a function of  $m_{\tilde{\chi}_1^0}$  for  $\tan\beta=7$  when  $\sigma_{\tilde{\chi}_1^0-p}$  takes on the maximum value of Fig.12[13].

For  $\mu < 0$  one again can get a cancelation reducing the cross section to a minimum near  $\tan\beta = 10$ :

$$\sigma_{\tilde{\chi}_1^0-p} \gtrsim 1 \times 10^{-12} \text{pb at } m_{1/2} = 600 \text{ GeV, } \tan\beta \cong 10, \mu < 0 \quad (24)$$

## 5 Conclusions

We have examined here the predictions of several SUGRA models which possess gauge coupling constant unification at  $M_G \cong 2 \times 10^{16}$  GeV, to see what parts of the SUSY parameter space are accessible to current detectors obeying Eq.(1), and what will be accessible to future detectors with the sensitivity of Eq.(2). For the minimal SUGRA model with universal soft breaking parameters, mSUGRA, current detectors are scanning parts of the parameter space where  $\tan\beta \gtrsim 25$ ,  $m_{\tilde{\chi}_1^0} \lesssim 90$  GeV and  $\Omega h^2 \lesssim 0.1$ . In addition, the light Higgs obeys  $m_h \lesssim 120$  GeV, and hence possibly would be accessible to RUN2 at the Tevatron. For nonuniversal models, where one allows the Higgs and third generation squark and slepton softbreaking masses to be nonuniversal, the neutralino-proton cross section can be significantly increased, by a factor of 10-100, with an appropriate choice of sign in the soft breaking deviations from universality. Thus current detectors here could scan regions of parameter space as low as  $\tan\beta \simeq 4$ , though in these regions  $m_h$  is very light, and the the minimum allowed  $\tan\beta$  may have to be raised as LEP raises the the bound on the Higgs mass. However, the possibility of large cross section here has already allowed current detectors to exclude parts of the high  $\tan\beta$  region, e.g. when  $\tan\beta \gtrsim 15$ . How low SUGRA cross sections can lie is complicated by the existance of coannihilation effects where the R-sleptons (particularly the  $\tilde{\tau}_1$ ) can become nearly degenerate with the neutralino. This allows the relic density constraint Eq.(4) to be satisfied in a narrow rising corridor (about 25 GeV wide in  $m_0$ ) in the  $m_0 - m_{1/2}$  plane rising to relatively large  $m_0$ , and thus reducing the size of the  $\tilde{\chi}_1^0 - p$  cross section. For large  $\tan\beta$ , the effect is sensitive to the value of  $A_0$ , the range of  $m_0$  increasing with  $A_0$ . Thus for  $\mu > 0$ , one finds for  $m_{1/2} = 600$  GeV, the minimum cross section at e.g.  $\tan\beta = 40$ ,  $A_0 = 4m_{1/2}$  is almost the same as that at  $\tan\beta = 3$ , the increase of the cross section due to the increase in  $\tan\beta$  being offset by the decrease due to the allowed large value of  $m_0$ . One finds however, that for  $\mu > 0$ , at  $m_{1/2} = 600$  GeV ( $m_{\tilde{g}} \cong 1.5$  TeV), the minimum cross sections would still be accessible to detectors with the sensitivity of Eq.(2). The minimum cross sections for  $\mu < 0$  is complicated by the possibility of accidental cancelations in the scattering amplitudes, allowing the cross section to sink below  $10^{-10}$  pb in certain regions of the parameter space. Thus one finds for mSUGRA that  $\sigma_{\tilde{\chi}_1^0 - p} < 1 \times 10^{-10}$  pb for  $m_{1/2} \gtrsim 450$  GeV ( $m_{\tilde{g}} \gtrsim 1.1$  TeV) when  $4 \lesssim \tan\beta \lesssim 20$ , with a minmum cross section of  $1 \times 10^{-12}$  pb reached at  $\tan\beta \cong 10$ . Similar results hold for the nonuniversal models. In this domain SUGRA models imply that halo dark matter would not be accessible to detectors with sensitivities of Eq.(2), and that the gluino and squarks would be quite heavy. They would still however be observable at the LHC which can detect gluinos with mass  $m_{\tilde{g}} \lesssim 2.5$  TeV [16].

## 6 Acknowledgement

This work was supported in part by National Science Foundation Grant No. PHY-9722090.

## References

1. A.H. Chamseddine, R. Arnowitt, P. Nath: Phys. Rev. Lett. **49**, 970 (1982); R. Barbieri, S. Ferrara, C.A. Savoy: Phys. Lett. B **119**, 343 (1982); L. Hall, J. Lykken, S. Weinberg: Phys. Rev. D **27**, 2359 (1983); P. Nath, R. Arnowitt, A.H. Chamseddine: Nucl. Phys. B **227**, 121 (1983).
2. For previous analysis of nonuniversal models see: V. Berezhinsky, A. Bottino, J. Ellis, N. Fornengo, G. Mignola, S. Scopel: Astropart. Phys. **5**, 1 (1996); Astropart. Phys. **6**, 333 (1996); P. Nath, R. Arnowitt: Phys. Rev. D **56**, 2820 (1997); R. Arnowitt, P. Nath: Phys. Lett. B **437**, 344 (1998); A. Bottino, F. Donato, N. Fornengo, S. Scopel: Phys. Rev. D **59**, 095004 (1999); R. Arnowitt, P. Nath: Phys. Rev. D **60**, 044002 (1999).
3. M. Alam et al.: Phys. Rev. Lett. **74**, 2885 (1995).
4. S. Bertolini, F. Borzumati, A. Masiero, G. Ridolfi: Nucl. Phys. B **353**, 591 (1991).
5. H. Anlauf: Nucl. Phys. B **430**, 245 (1994); M. Chiuchini, G. Deggrassi, P. Gambino, G.F. Giudice: Nucl. Phys. B **527**, 21 (1998); Nucl. Phys. B **534**, 3 (1998).
6. M. Carena, D. Garcia, U. Nierste, C.E.M. Wagner: hep-ph/0010003; G. Deggrassi, P. Gambino, G.F. Giudice: hep-ph/0009337.
7. R. Arnowitt, B. Dutta, Y. Santoso: *Coannihilation in SUGRA and D-Brane Models*, in preparation.
8. M.B. Green, J.H. Schwarz, E. Witten: *Superstring theory*, vol. 2. (Cambridge University Press, 1987)
9. J. Ellis, R. Flores: Phys. Lett. B **263**, 259 (1991); Phys. Lett. B **300**, 175 (1993).
10. M. Olsson: Phys. Lett. B **482**, 50 (2000); M. Pavan, R. Arndt, I. Strakovsky, R. Workman: nucl-th/9912034, *Proc. of 8th International Symposium on Meson-Nucleon Physics and Structure of Nucleon*, Zuoz, Switzerland, Aug., (1999).
11. A. Bottino, F. Donato, N. Fornengo, S. Scopel: Astropart. Phys. **13**, 215 (2000).
12. H. Leutwyler: Phys. Lett. B **374**, 163 (1996).
13. E. Accomando, R. Arnowitt, B. Dutta, Y. Santoso: Nucl. Phys. B **585**, 124 (2000).
14. J. Ellis, T. Falk, K. Olive, M. Srednicki: Astropart. Phys. **13**, 181 (2000).
15. J. Ellis, A. Ferstl, K. Olive: Phys. Lett. B **481**, 304 (2000).
16. ATLAS: *Detector and Physics Performance Technical Design Report*, vol. 1, CERN-LHCC-99-14, ATLAS-TDR-14 (1999); vol. 2, CERN-LHCC-99-15, ATLAS-TDR-15 (1999).